

Acid sphingomyelinase–ceramide system mediates effects of antidepressant drugs

Erich Gulbins^{1,2}, Monica Palmada¹, Martin Reichel³, Anja Lüth⁴, Christoph Böhmer¹, Davide Amato³, Christian P Müller³, Carsten H Tischbirek³, Teja W Groemer³, Ghazaleh Tabatabai^{5,6}, Katrin A Becker¹, Philipp Tripal³, Sven Staedtler³, Teresa F Ackermann⁷, Johannes van Brederode⁸, Christian Alzheimer⁸, Michael Weller⁵, Undine E Lang⁹, Burkhard Kleuser⁴, Heike Grassmé¹ & Johannes Kornhuber³

Major depression is a highly prevalent severe mood disorder that is treated with antidepressants. The molecular targets of antidepressants require definition. We investigated the role of the acid sphingomyelinase (Asm)-ceramide system as a target for antidepressants. Therapeutic concentrations of the antidepressants amitriptyline and fluoxetine reduced Asm activity and ceramide concentrations in the hippocampus, increased neuronal proliferation, maturation and survival and improved behavior in mouse models of stress-induced depression. Genetic Asm deficiency abrogated these effects. Mice overexpressing Asm, heterozygous for acid ceramidase, treated with blockers of ceramide metabolism or directly injected with C16 ceramide in the hippocampus had higher ceramide concentrations and lower rates of neuronal proliferation, maturation and survival compared with controls and showed depression-like behavior even in the absence of stress. The decrease of ceramide abundance achieved by antidepressant-mediated inhibition of Asm normalized these effects. Lowering ceramide abundance may thus be a central goal for the future development of antidepressants.

Major depression is a severe, chronic and often life-threatening illness with a lifetime prevalence of more than 10% (ref. 1). Key symptoms of depression include depressed mood, loss of interest and pleasure, feelings of worthlessness, weight loss and insomnia, and a high suicide risk². The disease may be triggered by psychological stress, inflammatory cytokines and dysfunction of the hypothalamic-pituitary-adrenal axis, among other causes^{1–4}.

The previously held hypothesis that antidepressants act by inhibition of monoamine uptake has been questioned because the antidepressant effect of these drugs is not clearly associated with their monoaminergic effect; in fact, the antidepressant tianeptine is actually a serotonin reuptake enhancer⁵. Furthermore, the direct effect

on monoamines contrasts with the delay of antidepressant effects in patients. Recent theories on the pathogenesis of major depression suggest a change of cellular plasticity predominantly in the hippocampus and a shift in the balance between neurogenic and antiapoptotic events that leads to neurodegeneration and hippocampal atrophy^{6–9}. Antidepressants increase neurogenesis and reverse hippocampal atrophy associated with major depression⁹.

Here, we investigated the role of the acid sphingomyelinase (here referred to as ASM for human protein and Asm for mouse protein) and ceramide system as a target for antidepressants. Asm is ubiquitously expressed and releases ceramide from sphingomyelin, predominantly in lysosomes but also in secretory lysosomes and on the plasma membrane^{10–13}.

The antidepressants amitriptyline, a tricyclic drug, and fluoxetine, a selective serotonin reuptake inhibitor, inhibited ASM activity in cultured neurons at therapeutic plasma concentrations recommended for patients with major depression¹⁴ (Fig. 1a). Treatment of wild-type (WT) mice with amitriptyline or fluoxetine dose-dependently reduced hippocampal Asm activity and protein amounts (Fig. 1b,c, Supplementary Fig. 1a,b,d and Supplementary Note 1), a finding consistent with the induction of partial proteolysis of Asm by amitriptyline and fluoxetine^{15,16}. Mice transgenic for Asm (t-Asm) showed higher Asm activity and protein amounts in the hippocampus than did WT mice, and treatment with amitriptyline and fluoxetine reduced Asm activity and protein amounts in WT and t-Asm mice (Fig. 1b and Supplementary Fig. 1a,c,d). We used Asm-deficient mice as specificity controls for the antibody to Asm (Supplementary Fig. 1a).

The reduction of Asm amounts and activity by amitriptyline or fluoxetine resulted in a dose-dependent reduction of ceramide abundance in the hippocampus of WT and t-Asm mice, as determined by diacylglycerol kinase assays (Fig. 1d), mass spectrometry (Supplementary Fig. 2a) and fluorescence microscopy (Fig. 1e and

¹Department of Molecular Biology, University of Duisburg-Essen, Essen, Germany. ²Department of Surgery, University of Cincinnati, Cincinnati, USA. ³Department of Psychiatry and Psychotherapy, Friedrich-Alexander-University of Erlangen-Nuremberg, Erlangen, Germany. ⁴Institute of Nutritional Sciences, University of Potsdam, Potsdam, Germany. ⁵Department of Neurology, University Hospital Zurich, Zurich, Switzerland. ⁶Neuroscience Center Zurich, Zurich, Switzerland. ⁷Department of Physiology I, University of Tübingen, Tübingen, Germany. ⁸Institute of Physiology and Pathophysiology, Friedrich-Alexander-University of Erlangen-Nuremberg, Erlangen, Germany. ⁹Department of Psychiatry and Psychotherapy, University Hospital Basel, Basel, Switzerland. Correspondence should be addressed to E.G. (erich.gulbins@uni-due.de) or J.K. (johannes.kornhuber@uk-erlangen.de).

Received 26 November 2012; accepted 23 April 2013; published online 16 June 2013; doi:10.1038/nm.3214

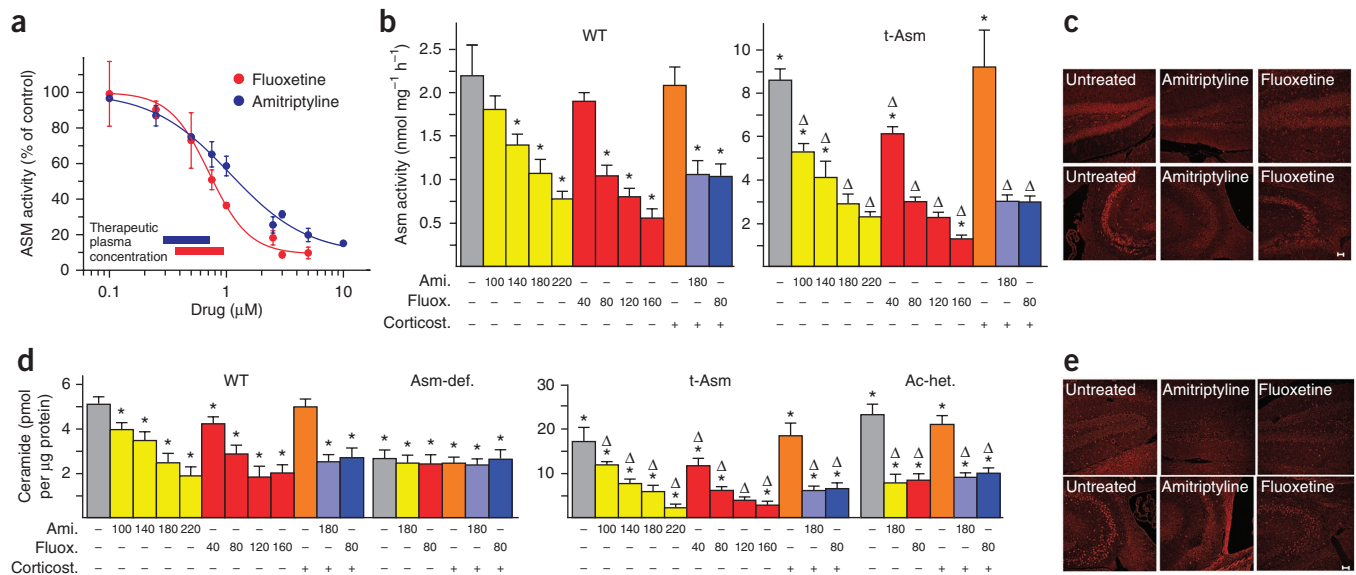


Figure 1 Amitriptyline and fluoxetine reduce hippocampal ceramide concentrations by inhibiting Asm activity. **(a)** ASM activity in human H4 neural cells at different concentrations of amitriptyline or fluoxetine. Therapeutic plasma concentrations of the antidepressants are indicated. Data are expressed as means \pm s.d. Results are representative of three independent experiments. **(b)** Effects of amitriptyline (Ami.) and fluoxetine (Fluox.) on Asm activity in the hippocampus of WT and t-Asm mice. Data are expressed as means \pm s.d. from WT mice ($n = 6$ – 12 per group) and t-Asm mice ($n = 6$ – 8 per group). Doses of amitriptyline and fluoxetine are given in mg L^{-1} . * $P < 0.05$ compared to untreated WT mice, $\Delta P < 0.05$ compared to untreated t-Asm mice, analysis of variance (ANOVA). **(c)** Immunostainings of hippocampal sections using Cy3-coupled antibodies against Asm showing expression of Asm in the dentate gyrus (top images) and CA3 region (bottom images) of untreated and amitriptyline- or fluoxetine-treated mice. Representative results from 9–12 mice per group, magnification $\times 200$. **(d)** Ceramide abundance in unstressed or corticosterone (Corticost.)-stressed mice that were treated with amitriptyline and fluoxetine or left untreated. Doses of amitriptyline and fluoxetine are given in mg L^{-1} . Data are expressed as means \pm s.d. (180 mg L^{-1} amitriptyline and 80 mg L^{-1} fluoxetine: WT and Asm-deficient (Asm-def.) mice, $n = 12$, t-Asm mice, $n = 9$. All other doses: $n = 5$. Ac-heterozygous (Ac-het.) mice, $n = 4$). * $P < 0.05$ compared to untreated WT mice, $\Delta P < 0.05$ compared to the corresponding untreated mice, ANOVA. **(e)** Immunostainings of hippocampal sections with Cy3-coupled antibodies against ceramide showing amount of ceramide in the dentate gyrus (upper) and CA3 regions (lower) after treatment of WT mice with amitriptyline or fluoxetine. Representative images from 12 mice each. Scale bars, 50 μm .

Supplementary Fig. 2b–e,h). In contrast, the antidepressants did not alter hippocampal ceramide abundance in Asm-deficient mice (Fig. 1d and Supplementary Fig. 2a–c,f,h). Constitutive hippocampal ceramide concentrations were lower in Asm-deficient mice and higher in t-Asm mice compared with WT mice (Fig. 1d and Supplementary Fig. 2a–c).

To increase constitutive hippocampal ceramide concentrations independent of Asm, we generated acid ceramidase-heterozygous (Ac-heterozygous) mice, which showed approximately 50% loss of acid ceramidase activity (data not shown) and very high concentrations of ceramide in the hippocampus; these concentrations were reduced by antidepressants (Fig. 1d and Supplementary Fig. 2a–c,g,h).

Because major depression has been linked to stress¹, we tested the effects of corticosterone, a well-established stress inducer (Supplementary Note 2), on Asm and ceramide. Corticosterone did not affect Asm activity or expression or ceramide concentrations (Fig. 1b,d and Supplementary Fig. 2a,i–n).

Next, we determined whether inhibition of Asm mediates effects of amitriptyline and fluoxetine on neurogenesis, neuronal maturation and survival. There was less neurogenesis, neuronal maturation and neuronal survival in t-Asm and Ac-heterozygous mice than in WT mice but more in Asm-deficient mice than in WT mice, even in the absence of any treatment (Fig. 2a–c and Supplementary Fig. 3a–d). Amitriptyline and fluoxetine increased neurogenesis, neuronal maturation and survival in the hippocampus of stressed or nonstressed WT, t-Asm and Ac-heterozygous mice, but did not do so in Asm-deficient mice (Fig. 2a–c and Supplementary Fig. 3a). Hippocampal

structural synaptic parameters did not differ between WT, Asm-deficient and t-Asm mice (Supplementary Fig. 4a,d). Furthermore, electrophysiological parameters were not different in CA3 pyramidal neurons of t-Asm mice when compared to WT mice and were independent of treatment with fluoxetine (Supplementary Fig. 4b,c). Ceramide reduced Akt phosphorylation at Ser473, which was increased by antidepressants (Fig. 2d). C16 ceramide also inhibited proliferation of PC12 cells, an effect that was abrogated by expression of the constitutively active T308DS473DAkt1 mutant of Akt1 (Supplementary Fig. 5).

Previous studies have shown that fluoxetine elicits egg laying in *Caenorhabditis elegans*; this egg laying is independent of the serotonin transporter Mod-5, and even *C. elegans* mutants that lack the receptors 1 (SER-1) and 2 (SER-4) for 5-hydroxytryptamine (5-HT), a system that would be targeted by antidepressants according to the monoamine hypothesis of antidepressant actions, at least partially respond to fluoxetine^{17,18}. To confirm our hypothesis that the Asm-ceramide system has a key role in the effect of antidepressants, we determined the effect of fluoxetine on egg laying in WT and *asm-1*-deficient *C. elegans* (Fig. 2e). Fluoxetine induced egg laying in WT *C. elegans*, but not in *asm-1*-deficient *C. elegans*. 5-HT still induced egg laying in *asm-1*-deficient worms, and deletion of Mod-5, the only serotonin transporter expressed in *C. elegans*, did not alter the effects of fluoxetine, indicating that the 5-HT system is independent or at least partially downstream of *asm-1* (Fig. 2e and Supplementary Figs. 6 and 7a,b).

To further substantiate the role of the Asm-ceramide system as a target for antidepressants, we tested whether fenflidine, a functional

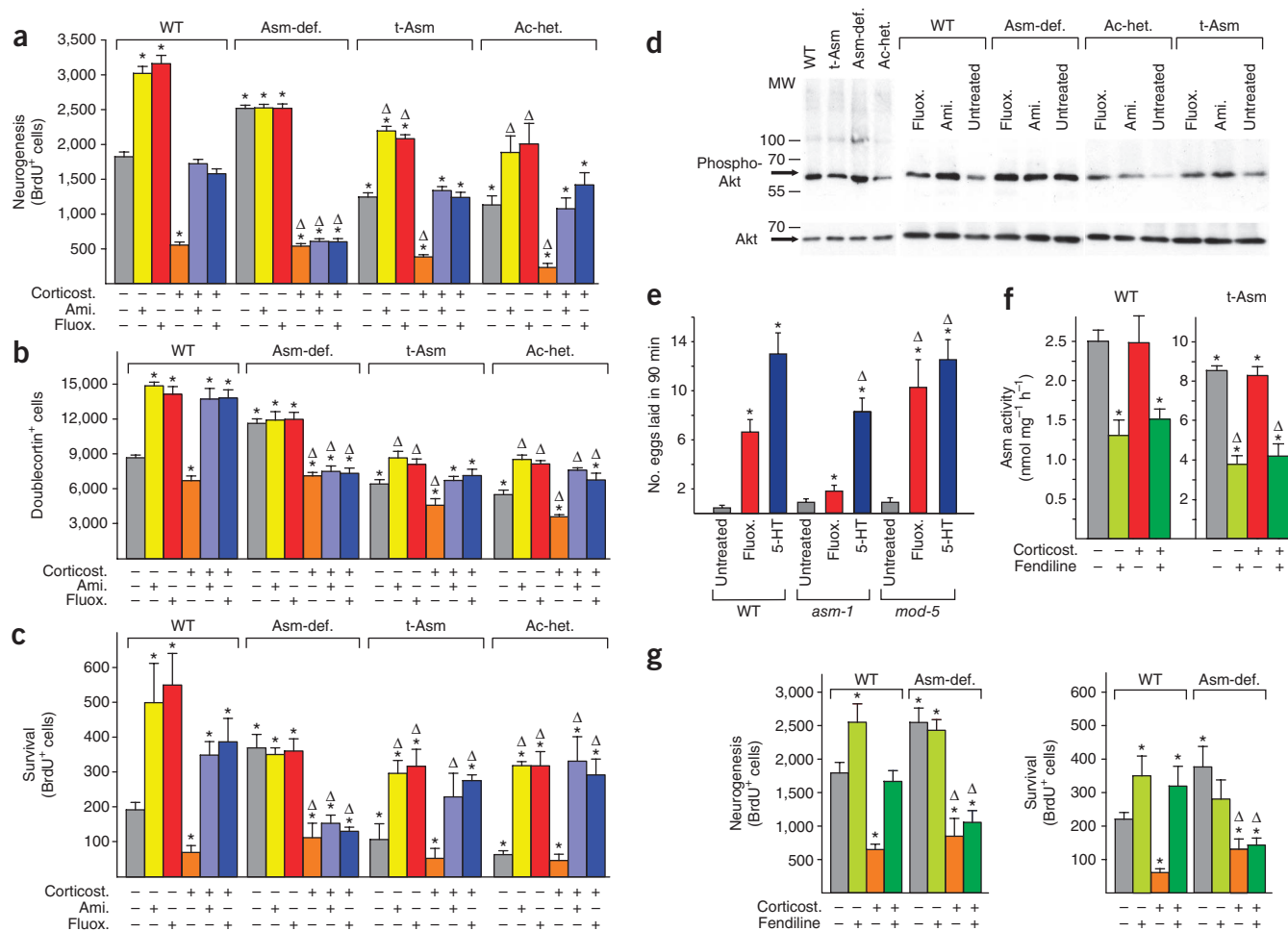


Figure 2 The Asm-ceramide system is required for the neurobiological effects of antidepressants. (**a–c**) Neurogenesis (**a**), neuronal maturation (**b**), and neuronal survival (**c**) in the hippocampus of unstressed or corticosterone-stressed mice that were treated with amitriptyline or fluoxetine. Data are expressed as means \pm s.d. (WT, t-Asm and Asm-deficient mice in **a**: $n = 12$; WT, t-Asm and Asm-deficient mice in **b** and **c**: $n = 6$; Ac-heterozygous mice: $n = 5$). * $P < 0.05$ compared to untreated WT mice, $\Delta P < 0.05$ compared to corresponding mice, ANOVA). (**d**) Western blots showing constitutive and antidepressant-induced phosphorylation of Ser 473 of Akt. Aliquots of the samples were blotted with antibodies against Akt (bottom blots). The blots are representative of results from four to six mice per group. (**e**) Fluoxetine- and 5-HT-induced egg laying in WT, *asm-1*-deficient and *mod-5*-deficient *C. elegans*. Data are expressed as means \pm s.d. from six to eight worms per group. * $P < 0.05$ compared to untreated WT worms, $\Delta P < 0.05$ compared to untreated corresponding genotype, ANOVA. (**f,g**) Asm activity and effects on neurogenesis and neuronal survival in nonstressed and stressed mice treated with fendiline or left untreated. Data are expressed as means \pm s.d. from six (**f** and neurogenesis) or four (neuronal survival) mice. * $P < 0.05$ compared to untreated WT mice, $\Delta P < 0.05$ compared to untreated Asm-deficient mice, ANOVA.

inhibitor of ASM¹⁶ that has not been reported to be an antidepressant, can also act as antidepressant. Fendiline reduced Asm activity and reduced ceramide concentrations in the hippocampus in WT and t-Asm mice (Fig. 2f, Supplementary Fig. 8a and Supplementary Note 3). This resulted in increased neurogenesis, neuronal maturation and neuronal survival in WT but not Asm-deficient mice, very similar to the effects of amitriptyline and fluoxetine (Fig. 2g, Supplementary Fig. 8b–d and Supplementary Note 3). Abundance of ceramide in the hippocampus of t-Asm mice and Ac-heterozygous mice was associated with depression-like behavior (Fig. 3a–f and Supplementary Fig. 9). Treatment with antidepressants or fendiline normalized this depression-like behavior. In contrast, Asm-deficient mice showed constitutively reduced depression-like behavior and, notably, antidepressants or fendiline had no effect on depression-like behavior of Asm-deficient mice (Fig. 3a–f and Supplementary Fig. 9). Corticosterone application resulted in severe depressive-like behavior in all mouse types (Fig. 3a–f and Supplementary Fig. 9). Treatment with antidepressants or fendiline

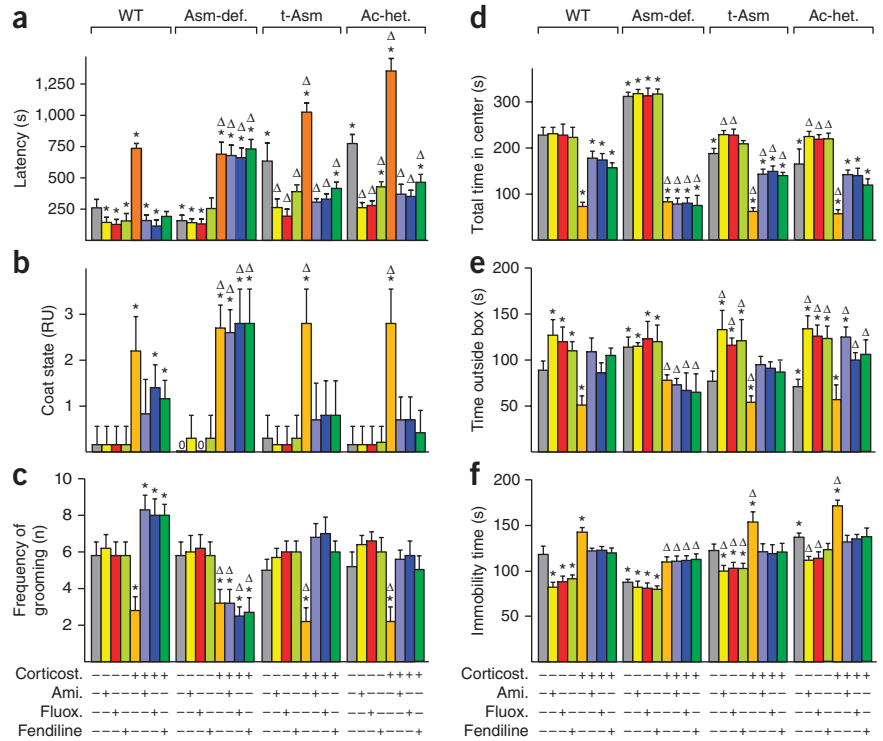
attenuated the corticosterone-induced depressive-like behavior in WT, t-Asm and Ac-heterozygous mice but had no effect on corticosterone-induced depressive-like behavior in Asm-deficient mice (Fig. 3a–f and Supplementary Fig. 9). These findings indicate that several behavioral effects of antidepressants and fendiline depend on the presence of Asm and are mediated by a reduction of ceramide concentrations.

To further compare the roles of ceramide and Asm in major depression, we increased the amount of ceramide in the hippocampus independent of Asm and acid ceramidase by administering the glycosyltransferase inhibitor D,L-threo-1-phenyl-2-decanoylamino-3-morpholino-1-propanol (PDMP), which prevents glycosylation of ceramide and has been shown to increase ceramide concentrations in gerbil hippocampus and cells^{19,20}. PDMP treatment doubled ceramide concentrations, decreased neurogenesis and neuronal maturation in the hippocampus and induced depression-like symptoms in WT and Asm-deficient mice (Fig. 4a,b and Supplementary Fig. 10a–g). These alterations were corrected in WT mice by treatment with amitriptyline

Figure 3 Behavioral effects of antidepressant drugs can be mediated by the inhibition of acid sphingomyelinase. (a–f) Novelty-suppressed feeding (a), coat (b), splash (c), open-field (d), light-dark box (e) and forced-swim (f) tests in nonstressed and corticosterone-stressed mice treated with antidepressants, fendiline or left untreated. RU, relative units. Data are expressed as means \pm s.d. Number of mice per group in a from left to right: 41, 42, 19, 9, 12, 12, 12, 9, 33, 28, 14, 9, 12, 12, 12, 8, 19, 14, 12, 10, 12, 12, 12 and 10. In all other panels, WT, Asm-deficient and t-Asm mice $n = 6$. Ac-heterozygous mice $n = 5$. * $P < 0.05$ compared to untreated WT mice, $\Delta P < 0.05$ compared to untreated control of each genotype, ANOVA.

or fluoxetine, whereas the antidepressants had no effects in Asm-deficient mice treated with PDMP (Fig. 4a,b and Supplementary Fig. 10a–g). Further, reduction of ceramide abundance in Ac-heterozygous mice by heterozygosity of Asm normalized neurogenesis, maturation and depression-like behavior (Fig. 4a,b and Supplementary Fig. 10a–g). Finally, we injected C16 ceramide directly into the hippocampus of WT mice, which induced depression-like symptoms, whereas solvent controls had no effect (Fig. 4c and Supplementary Fig. 10h).

To investigate the role of the Asm-ceramide system in the effects of antidepressants in a different stress model, we used the chronic unpredictable stress model. Chronic unpredictable stress increased ceramide concentrations approximately twofold in the hippocampus of both WT and Asm-deficient mice and concomitantly reduced neurogenesis and neuronal maturation (Fig. 4d,e), events that were normalized by antidepressants in WT mice, but not in Asm-deficient mice.



Major depression is a common, complex and probably multifactorial psychiatric disorder. Here we propose a previously unknown mode of action for antidepressants (Supplementary Fig. 11). Ceramide acts as a negative regulator in the multifactorial pathogenesis of major depression. Inhibiting Asm activity reduces hippocampal ceramide concentrations and permits normalization of behavior, neurogenesis, neuronal maturation and neuronal survival.

Ceramide may regulate neurogenesis through several pathways. It controls activity of Akt that has been shown to be important for neuronal proliferation²¹. It has been also shown to regulate the

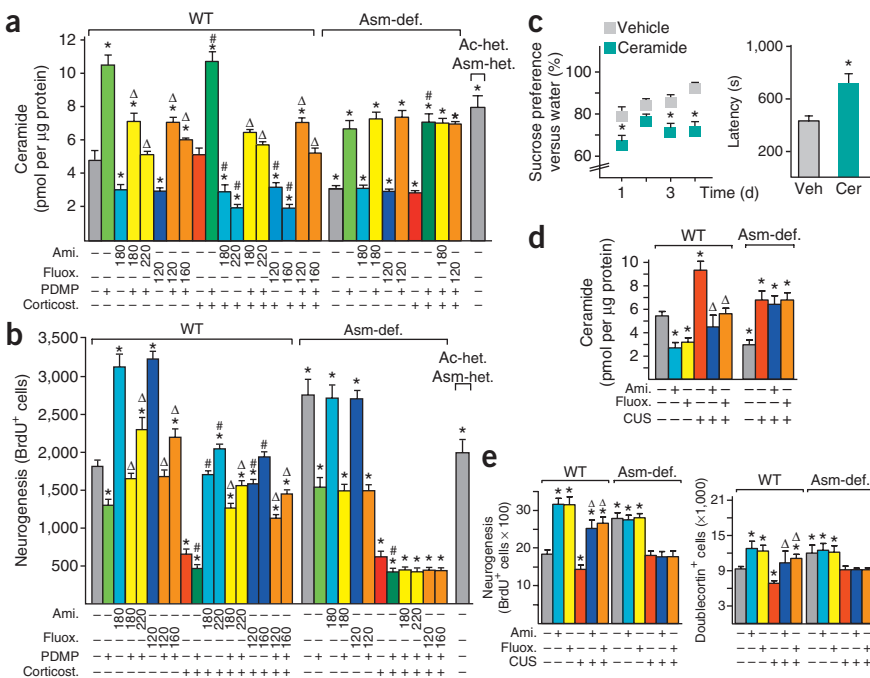


Figure 4 Hippocampal ceramide has a crucial role in depression-like phenotypes. (a,b) Ceramide levels (a) and neurogenesis (b) in unstressed or corticosterone-stressed mice treated with PDMP and/or amitriptyline or fluoxetine. Doses of amitriptyline and fluoxetine are given in mg L⁻¹. Data are expressed as means \pm s.d. from five mice each. * $P < 0.05$ compared to untreated WT mice, $\Delta P < 0.05$ compared to PDMP alone or corticosterone + PDMP as appropriate; # $P < 0.05$ compared to corticosterone alone as appropriate, ANOVA. (c) Effects of injection of C16 ceramide (Cer) into the hippocampus on depression-like behavior in mice. Data are expressed as means \pm s.e.m. from five mice for vehicle-treated control (Veh) and eight mice for Cer. * $P < 0.05$, two-tailed t -test. (d,e) Hippocampal ceramide, neurogenesis and maturation in WT and Asm-deficient mice subjected to chronic unpredictable stress (CUS) and treated with amitriptyline or fluoxetine or left untreated. Data are expressed as means \pm s.d. from five mice each. * $P < 0.05$ compared to untreated WT mice, $\Delta P < 0.05$ compared to CUS-treated mice of each genotype, ANOVA.



formation of reactive oxygen species through activation of NADPH oxidases²², to mediate the effects of the cytokines interleukin-1 β and tumor necrosis factor- α ^{23–25} and to regulate stress-activated kinases²⁶ and calcium release²⁷. Thus, ceramide may coordinate negative effects on hippocampal neurons by Akt inhibition and assembly of molecules involved in oxidative stress, proinflammatory receptors and stress signaling. Antidepressants counteract these events by reducing ceramide levels. This view is consistent with the finding that patients with major depression experience a wide range of abnormalities in organs such as heart, bone and blood, in which oxidative stress, proinflammatory cytokines and sphingolipids are elevated^{28–32}. These pathologic conditions might be explained by the increased ceramide concentration in major depression, not only in hippocampal neurons but also in other cells³³.

We therefore propose that ASM is a key target of antidepressant drugs in the hippocampus. We suggest that cellular ceramide concentration may be a previously unknown mediator of hippocampal functions, including neurogenesis and neuronal networks that determine behavior.

METHODS

Methods and any associated references are available in the [online version of the paper](#).

Note: Supplementary information is available in the [online version of the paper](#).

ACKNOWLEDGMENTS

Asm-deficient mice and *asm-1*-deficient worms were provided by R. Kolesnick, Memorial Sloan Kettering Cancer Hospital, and E2A-Cre mice by R. Waldschütz, University Hospital Essen. The G4 antibody against Asm was provided by K. Sandhoff, University of Bonn. We thank S. Harde, B. Wilker, C. Sehl, S. Keitsch, M. Schäfer, S. Müller and E. Naschberger for excellent technical help and F. Lang for valuable discussion. Parts of the work were supported by funding from Deutsche Forschungsgemeinschaft grants GU 335/23-1, KO 947/11-1 and GRK 1302.

AUTHOR CONTRIBUTIONS

E.G. and J.K. initiated the studies, designed experiments and supervised research. E.G., J.K. and M.W. wrote the manuscript. E.G. also performed most mouse studies. E.G., K.A.B. and G.T. performed the histological studies and developed the polyclonal Asm-specific antibody. M.P. and C.B. performed the *C. elegans* studies. A.L. and B.K. measured ceramide concentrations by mass spectrometry. M.W. designed some experiments and participated in BrdU stainings. H.G. performed the confocal microscopy studies. J.K., P.T. and S.S. performed experiments on the concentration-dependent inhibition of ASM by antidepressant drugs. M.R. and M.P. performed experiments on 5-HT uptake in cultured hippocampal neurons. M.R. and J.K. performed experiments on 5-HT uptake in mouse brain synaptosomes. C.H.T. and T.W.G. designed and performed synapse staining and confocal analyses. T.F.A., U.E.L. and E.G. performed behavioral experiments. C.P.M., D.A., M.R. and J.K. designed and performed hippocampal injection and microdialysis studies. C.A., J.v.B., M.R. and J.K. designed and performed electrophysiological studies in hippocampal slices. All authors discussed the results and commented on the manuscript.

COMPETING FINANCIAL INTERESTS

The authors declare no competing financial interests.

Reprints and permissions information is available online at <http://www.nature.com/reprints/index.html>.

1. Belmaker, R.H. & Agam, G. Major depressive disorder. *N. Engl. J. Med.* **358**, 55–68 (2008).
2. Howren, M.B., Lamkin, D.M. & Suls, J. Associations of depression with C-reactive protein, IL-1, and IL-6: a meta-analysis. *Psychosom. Med.* **71**, 171–186 (2009).
3. Dowlati, Y. *et al.* A meta-analysis of cytokines in major depression. *Biol. Psychiatry* **67**, 446–457 (2010).

4. Krishnan, V. & Nestler, E.J. The molecular neurobiology of depression. *Nature* **455**, 894–902 (2008).
5. Brink, C.B., Harvey, B.H. & Brand, L. Tianeptine: a novel atypical antidepressant that may provide new insights into the biomolecular basis of depression. *Recent Pat. CNS Drug Discov.* **1**, 29–41 (2006).
6. Santarelli, L. *et al.* Requirement of hippocampal neurogenesis for the behavioral effects of antidepressants. *Science* **301**, 805–809 (2003).
7. Koo, J.W. & Duman, R.S. IL-1 β is an essential mediator of the antineurogenic and anhedonic effects of stress. *Proc. Natl. Acad. Sci. USA* **105**, 751–756 (2008).
8. David, D.J. *et al.* Neurogenesis-dependent and -independent effects of fluoxetine in an animal model of anxiety/depression. *Neuron* **62**, 479–493 (2009).
9. Warner-Schmidt, J.L. & Duman, R.S. Hippocampal neurogenesis: opposing effects of stress and antidepressant treatment. *Hippocampus* **16**, 239–249 (2006).
10. Gulbins, E. & Kolesnick, R. Raft ceramide in molecular medicine. *Oncogene* **22**, 7070–7077 (2003).
11. Grassmé, H. *et al.* CD95 signaling via ceramide-rich membrane rafts. *J. Biol. Chem.* **276**, 20589–20596 (2001).
12. Perrotta, C. *et al.* Syntaxin 4 is required for acid sphingomyelinase activity and apoptotic function. *J. Biol. Chem.* **285**, 40240–40251 (2010).
13. Grassmé, H. *et al.* Host defense against *Pseudomonas aeruginosa* requires ceramide-rich membrane rafts. *Nat. Med.* **9**, 322–330 (2003).
14. Baumann, P. *et al.* The AGNP-TDM Expert Group Consensus Guidelines: focus on therapeutic monitoring of antidepressants. *Dialogues Clin. Neurosci.* **7**, 231–247 (2005).
15. Kölzer, M., Werth, N. & Sandhoff, K. Interactions of acid sphingomyelinase and lipid bilayers in the presence of the tricyclic antidepressant desipramine. *FEBS Lett.* **559**, 96–98 (2004).
16. Kornhuber, J. *et al.* Identification of new functional inhibitors of acid sphingomyelinase using a structure-property-activity relation model. *J. Med. Chem.* **51**, 219–237 (2008).
17. Ranganathan, R., Sawin, E.R., Trent, C. & Horvitz, H.R. Mutations in the *Caenorhabditis elegans* serotonin reuptake transporter MOD-5 reveal serotonin-independent and -independent activities of fluoxetine. *J. Neurosci.* **21**, 5871–5884 (2001).
18. Dempsey, C.M., Mackenzie, S.M., Gargus, A., Blanco, G. & Sze, J.Y. Serotonin (5HT), fluoxetine, imipramine and dopamine target distinct 5HT receptor signaling to modulate *Caenorhabditis elegans* egg-laying behavior. *Genetics* **169**, 1425–1436 (2005).
19. De Stefanis, D. *et al.* Increase in ceramide level alters the lysosomal targeting of cathepsin D prior to onset of apoptosis in HT-29 colon cancer cells. *Biol. Chem.* **383**, 989–999 (2002).
20. Hisaki, H. *et al.* *In vivo* influence of ceramide accumulation induced by treatment with a glucosylceramide synthase inhibitor on ischemic neuronal cell death. *Brain Res.* **1018**, 73–77 (2004).
21. Peltier, J., O'Neill, A. & Schaffer, D.V. PI3K and CREB regulate adult neural hippocampal progenitor proliferation and differentiation. *Dev. Neurobiol.* **67**, 1348–1361 (2007).
22. Zhang, Y., Li, X., Carpinteiro, A. & Gulbins, E. Acid sphingomyelinase amplifies redox signaling in *Pseudomonas aeruginosa*-induced macrophage apoptosis. *J. Immunol.* **181**, 4247–4254 (2008).
23. Mathias, S. *et al.* Activation of the sphingomyelin signaling pathway in intact EL4 cells and in a cell-free system by IL-1 β . *Science* **259**, 519–522 (1993).
24. Wiegmann, K., Schütze, S., Machleidt, T., Witte, D. & Krönke, M. Functional dichotomy of neutral and acidic sphingomyelinases in tumor necrosis factor signaling. *Cell* **78**, 1005–1015 (1994).
25. Kim, M.Y., Linardic, C., Obeid, L. & Hannun, Y. Identification of sphingomyelin turnover as an effector mechanism for the action of tumor necrosis factor α and γ -interferon. Specific role in cell differentiation. *J. Biol. Chem.* **266**, 484–489 (1991).
26. Brenner, B. *et al.* Fas- or ceramide-induced apoptosis is mediated by a Rac1-regulated activation of Jun N-terminal kinase/p38 kinases and GADD153. *J. Biol. Chem.* **272**, 22173–22181 (1997).
27. Lepple-Wienhues, A. *et al.* Stimulation of CD95 (Fas) blocks T lymphocyte calcium channels through sphingomyelinase and sphingolipids. *Proc. Natl. Acad. Sci. USA* **96**, 13795–13800 (1999).
28. Müller, N. COX-2 inhibitors as antidepressants and antipsychotics: clinical evidence. *Curr. Opin. Investig. Drugs* **11**, 31–42 (2010).
29. Walker, J.R. *et al.* Psychiatric disorders in patients with immune-mediated inflammatory diseases: prevalence, association with disease activity, and overall patient well-being. *J. Rheumatol. Suppl.* **88**, 31–35 (2011).
30. Rudisch, B. & Nemeroff, C.B. Epidemiology of comorbid coronary artery disease and depression. *Biol. Psychiatry* **54**, 227–240 (2003).
31. Kojima, M. *et al.* Depression, inflammation, and pain in patients with rheumatoid arthritis. *Arthritis Rheum.* **61**, 1018–1024 (2009).
32. Tabas, I. Sphingolipids and atherosclerosis: a mechanistic connection? A therapeutic opportunity? *Circulation* **110**, 3400–3401 (2004).
33. Kornhuber, J. *et al.* High activity of acid sphingomyelinase in major depression. *J. Neural Transm.* **112**, 1583–1590 (2005).

ONLINE METHODS

Mice and treatments. Asm-deficient mice (*Smpd1*^{-/-}) show age-dependent accumulation of sphingomyelin and development of Niemann-Pick syndrome A or B, depending on the residual activity of ASM³⁴. To avoid sphingomyelin accumulation, we used only *Smpd1*^{-/-} mice with a maximum age of 12 weeks³⁵. We observed no increase in cell death in the hippocampus of these mice (data not shown). In Asm transgenic mice, the mouse *Smpd1* cDNA was expressed under the control of the ubiquitous cytomegalovirus (CMV) immediate early enhancer/chicken β -actin fusion promoter. A *loxP*-flanked STOP cassette was included between the promoter and the transgene so that the expression could be conditionally regulated by the action of Cre recombinase. The conditional transgene was introduced into the deleted *Hprt* gene locus of embryonic day 14 embryonic stem cells. The transgenic mice were generated and backcrossed for at least five generations to C57BL/6 mice. The transgene was constitutively expressed by crossing these mice with mice expressing Cre recombinase under the control of an E2A promoter³⁶. For acid ceramidase 1 (*Asah1*)-heterozygous mice, the exon-intron organization of the gene was established on the basis of the *Asah1* cDNA sequence [NM_019734](#). A targeting vector containing regions homologous to genomic *Asah1* sequences was constructed. It included homology regions in the C57BL/6 genetic background, a long homology region of 5.8 kb and a short homology region of 1.7 kb, two *loxP* sites flanking *Asah1* exon 1, a neomycin gene flanked by flippase recognition target sites for positive selection, and a diphtheria toxin A negative-selection marker to reduce the isolation of nonhomologous recombined embryonic stem cell clones and to enhance the isolation of embryonic stem cell clones harboring the distal *loxP* site. This targeting vector was inserted into C57BL/6 embryonic stem cells by homologous recombination. Offspring were crossed with E2A-Cre mice to generate mice heterozygous for Ac. We used male and female mice. All studies were performed in accordance with animal permissions of the Landesumweltamt Nordrhein-Westfalen, Regierungspraesidium Tübingen and the Regierung von Mittelfranken. Amitriptyline (100, 140, 180 or 220 mg L⁻¹), fluoxetine (40, 80, 120 or 160 mg L⁻¹) or fendiline (17, 33, 67.5 or 135 mg L⁻¹) was administered for 35 d to mice through their drinking water. Drugs were dissolved in water, which was changed every 48 h. BrdU was injected at a dose of 75 mg per kg body weight four times (every 2 h) either 1 d or 21–28 d before the mice were killed. Corticosterone was administered at 0.25 mg mL⁻¹ in the drinking water for 28 d. If amitriptyline, fluoxetine and corticosterone were administered together, the corticosterone treatment was initiated 7 d after the initiation of antidepressant treatment.

In the chronic unpredictable stress model, the mice were challenged with unpredictable environmental stress for 5 weeks, including shift of the day-light cycle (four light-dark successions of 30 min every 24 h once a week), reversal of the light-dark cycle once a week, 3 h of 45° tilting of the cage twice a week, water deprivation for 14 h once a week and predator sounds (15 min) three times a week.

Plasma levels of antidepressant drugs. Plasma levels of amitriptyline were measured by high-performance liquid chromatography and those of fluoxetine and fendiline by liquid chromatography–tandem mass spectrometry.

Pharmacological inhibition of ASM activity *in vitro*. Human brain neuroglioma H4 cells (Promochem, Wesel, Germany) were cultured in DMEM with 10% FBS and 4 mM glutamine at 37 °C, 8.5% CO₂. H4 cells were grown to a confluence of 80–90%, incubated with amitriptyline, fluoxetine or fendiline at final concentrations from 0.1 to 10 μ M for 24 h and washed, and ASM activity was determined in whole-cell lysates^{11,16}.

Asm activity in mouse hippocampus. The hippocampal area was removed, shock frozen and lysed in 250 mM sodium acetate (pH 5.0), 1% NP40 and 1.3 mM EDTA for 15 min. The tissues were then homogenized by two rounds of sonication for 10 s each with a tip sonicator. Aliquots of the lysates were diluted to 250 mM sodium acetate (pH 5.0), 0.1% NP40 and 1.3 mM EDTA, then incubated with 50 nCi per sample [¹⁴C]sphingomyelin for 30 min at 37 °C and processed as above.

Measurement of ceramide by diacylglycerol kinase method. The hippocampal area was removed, homogenized in 200 μ L H₂O by tip sonication and extracted in CHCl₃/CH₃OH/1N HCl (100:100:1, v/v/v). The lower phase was collected, dried, resuspended in 20 μ L of a detergent solution (7.5% (w/v) *n*-octyl glucopyranoside, 5 mM cardiolipin in 1 mM diethylenetriaminepentaacetic acid (DTPA)) and sonicated for 10 min. The kinase reaction was started by the addition of 70 μ L of a reaction mixture containing 10 μ L diacylglycerol kinase (GE Healthcare Europe, Munich, Germany), 0.1 M imidazole/HCl (pH 6.6), 0.2 mM DTPA (pH 6.6), 70 mM NaCl, 17 mM MgCl₂, 1.4 mM ethylene glycol tetraacetic acid, 2 mM dithiothreitol, 1 μ M ATP and 5 μ Ci [³²P] γ ATP. The kinase reaction was performed for 30 min at room temperature and terminated by the addition of 1 mL CHCl₃/CH₃OH/1N HCl (100:100:1, v/v/v), 170 μ L buffered saline solution (135 mM NaCl, 1.5 mM CaCl₂, 0.5 mM MgCl₂, 5.6 mM glucose, 10 mM HEPES (pH 7.2)) and 30 μ L of a 100 mM EDTA solution. The lower phase was collected, dried and separated on Silica G60 thin-layer chromatography plates with chloroform/acetone/methanol/acetic acid/H₂O (50:20:15:10:5, v/v/v/v/v). The thin-layer chromatography plates were exposed to radiography films, the spots were removed from the plates and the incorporation of [³²P] into ceramide was measured by liquid scintillation counting. Ceramide amounts were determined by comparison with a standard curve using C16 to C24 ceramides as substrates.

Liquid chromatography–mass spectrometry analysis. The hippocampal area was removed and homogenized in 1 mL of methanol by tip sonication. Ceramides were extracted and 20 pmol of C17 ceramide in methanol were added as an internal standard, followed by the addition of 1 mL each of chloroform, distilled water and methanol. After 2 min of intensive stirring, 1 mL chloroform was added. The sample was stirred again for 2 min, and 1 mL of distilled water was added. The lower organic phase was collected, and the aqueous phase was extracted twice with 1 mL of chloroform. The combined organic phases were dried, lipids were resolved in 200 μ L of methanol and analyzed by rapid-resolution liquid chromatography–mass spectrometry (LC-MS) using an Agilent 1200 Series binary pump, a degasser and an autosampler (Agilent Technologies, Böblingen, Germany). A quadrupole time-of-flight 6530 mass spectrometer equipped with Jet-Stream technology operating in the positive electrospray ionization mode was used for detection (Agilent Technologies). High-purity nitrogen for the mass spectrometer was produced by a nitrogen generator (Parker Balston, Maidstone, UK). Chromatographic separations were obtained with a ZORBAX Eclipse XDB-C18 (C18, 4.6 \times 50 mm, 1.8 μ m particle size, 80 Å pore size; Agilent Technologies). The injection volume per sample was 10 μ L. An isocratic solvent system consisting of acetonitrile/2-propanol 3:2 (v/v) with 1% formic acid and a flow rate of 1 mL min⁻¹ over 15 min was used. For mass spectrometric measurements, the following ion source conditions and gas settings for positive LC-MS/MS were adjusted: sheath gas temperature, 400 °C; sheath gas flow, 9 L min⁻¹; nebulizer pressure, 30 psig; drying gas temperature, 350 °C; drying gas flow, 8 L min⁻¹; capillary voltage, 2,000 V; fragmentor voltage, 355 V; nozzle voltage, 2,000 V. All ceramides gave the same fragment ion of *m/z* 264.27 at various retention times, depending on their chain length. Counting was performed with Mass Hunter software. Calibration curves of reference ceramides were performed from 1–100 pmol and were constructed by linear fitting using the least-squares linear regression calculation. The resulting slope of the calibration curve was used to calculate the concentration of the respective analyte in the samples.

Immunohistochemical analysis of Asm and ceramide. Mice were euthanized and perfused through the left heart for 2 min with 0.9% NaCl and for 15 min with 4% paraformaldehyde (PFA) buffered in PBS (pH 7.3). Brains were removed, fixed for an additional 36 h in 4% buffered PFA in PBS and embedded in paraffin. The hippocampus was serially sectioned. The sections were dewaxed, incubated for 30 min with pepsin (Digest All, Invitrogen, Darmstadt, Germany) at 37 °C, washed and blocked for 10 min with PBS, 0.05% Tween 20 and 5% FCS (FCS). They were then immunostained for 45 min with a polyclonal rabbit antiserum containing antibodies to mouse Asm, obtained by immunization of rabbits with a purified GST fusion protein of mouse Asm (amino acids 518–564). The results were confirmed by staining with a monoclonal

antibody against Asm (provided by K. Sandhoff). Ceramide was detected with monoclonal antibody against ceramide (clone S58-9, Glycobiotech, Kükels, Germany). All antibodies were diluted 1:100 in HEPES/saline (132 mM NaCl, 20 mM HEPES [pH 7.4], 5 mM KCl, 1 mM CaCl₂, 0.7 mM MgCl₂, 0.8 mM MgSO₄) + 1% FCS, washed three times in PBS + 0.05% Tween 20, incubated for 45 min with Cy3-coupled donkey F(ab)₂ of antibodies specific for rabbit (anti-rabbit) IgG or mouse (anti-mouse) IgM (Jackson ImmunoResearch, Newmarket, UK), washed again three times in PBS + 0.05% Tween 20 and once in PBS, and embedded in Mowiol. Immunofluorescence was measured with the Leica TCS SL software program, version 2.61 (Leica, Mannheim, Germany).

Immunohistochemical BrdU, doublecortin, NeuN and GFAP stainings.

For BrdU staining, mice were injected with BrdU and killed, and brains were prepared as above. Paraffin-embedded sections were dewaxed, treated for 20 min with pepsin at 37 °C, washed, incubated for 2 h with 50% formamide in 300 mM NaCl and 30 mM saline sodium citrate (pH 7.0) at 65 °C and washed twice in saline sodium citrate buffer. The DNA was denatured for 30 min at 37 °C with 2 M HCl, washed, neutralized for 10 min with 0.1 M borate buffer (pH 8.5), washed and blocked with 0.05% Tween 20 and 5% FCS in PBS (pH 7.4). The samples were then stained with 5 µg mL⁻¹ BrdU-specific antibody (1:20, Roche 11170376001, Mannheim, Germany) for 45 min at 22 °C, washed and stained with Cy3-coupled F(ab)₂ fragments of antibody against mouse IgG (1:500, Jackson ImmunoResearch 715-166-150, Suffolk, UK). Serial sections were counted by a blinded investigator.

For doublecortin staining, the samples were demasked in citrate buffer after rehydration, incubated in a microwave for 15 min at 650 W, washed in PBS, blocked in blocking solution (Candor Biosciences, Wangen, Germany), stained with antibodies against doublecortin (1:100, Abcam Ab18723, Cambridge, UK) for 45 min at 22 °C, washed three times in PBS/0.05% Tween 20, stained with Cy3-coupled anti-rabbit IgG F(ab)₂ fragments (1:1,000, Jackson ImmunoResearch 711-166-152), washed again and embedded in Mowiol.

For BrdU-specific antibody and glial fibrillary acidic protein (GFAP) double stainings, after staining with BrdU-specific antibodies, the samples were incubated with antibodies for GFAP (1:1,000, Dako Z-0334, Eching, Germany) for 45 min at 22 °C, washed three times in PBS/0.05% Tween 20 and once in PBS, stained with FITC-conjugated anti-rabbit IgG F(ab)₂ fragments (1:1,000, Jackson ImmunoResearch 711-096-152) for 45 min at 22 °C, washed again and embedded in Mowiol.

For BrdU and NeuN double stainings, samples were processed as above for BrdU, incubated with BrdU-specific antibodies for 45 min at 22 °C, washed three times in PBS/0.05% Tween 20 and once in PBS, fixed for 15 min in 2% PFA/PBS (pH 7.3), washed four times with PBS, demasked in citrate buffer for 15 min in a microwave at 650 W, washed, blocked with PBS/0.05% Tween/5% FCS for 15 min, washed, incubated with antibodies against NeuN (1:100; Millipore MAB377, Schwalbach, Germany) for 45 min at 22 °C, washed three times in PBS/0.05% Tween 20 and once in PBS, stained with Cy3-coupled F(ab)₂ fragments of antibodies specific for rat IgG (1:100, Jackson ImmunoResearch 712-166-153) and FITC-conjugated anti-mouse IgG F(ab)₂ fragments (1:500, Jackson ImmunoResearch 715-096-150) for 45 min at 22 °C, washed and embedded.

Neurogenesis and neuronal survival were determined by BrdU labeling 1 d or 21–28 d before the mice were killed. Maturation was analyzed by doublecortin staining. Every tenth section of serial sections of the hippocampus was counted.

Western blots. The hippocampal area was removed, immediately shock frozen and homogenized with a tip sonicator in 100 µl 0.1% SDS, 25 mM HEPES, 0.5% deoxycholate, 0.1% Triton X-100, 10 mM EDTA, 10 mM sodium pyrophosphate, 10 mM sodium fluoride, 125 mM NaCl and 10 µg g⁻¹ hippocampus aprotinin/leupeptin. Samples were lysed for 5 min at 4 °C and centrifuged at 14,000 r.p.m. for 5 min at 4 °C, after which 20 µL 5× SDS-Laemmli buffer was added. Proteins were separated by 8.5% SDS-PAGE, incubated with either an antibody specific for phospho-Ser473 Akt or for Akt (both diluted 1:1,000, Cell Signaling 9271 and 9272, Frankfurt, Germany) for 1 h at 22 °C, washed and developed with alkaline phosphatase-coupled secondary antibodies (1:20,000, Santa Cruz Biotechnology, Inc. sc-2007, Heidelberg, Germany) with the Tropix chemoluminescence system.

Behavioral studies. Behavioral testing was performed between 3:00 p.m. and 6:00 p.m. If appropriate, mice were video tracked by a camera (Noldus-Systems, Worpsswede, Germany). All tests were performed on separate days. Experiments were performed with diffuse indirect room light. Novelty-suppressed feeding was measured as the length of time during which the mice explored a new environment before they began eating after a fasting period of 24 h. For the forced-swim test, mice were placed in a cylinder filled with water (21–23 °C) for 15 min. After 24 h, the mice were again placed in a water-filled cylinder for 6 min, and the time of mobility during the last 4 min of the second trial was recorded. Mice were judged immobile when they moved only to keep their heads above water. A quadratic open-field arena was used with sides 50 cm long, a white plastic floor and sidewalls 30 cm high. Each mouse was released near the wall and observed for 30 min. The open field was defined as 10 cm away from the wall. The light-dark box test consisted of a dark and safe compartment and a brightly illuminated, open, and thus aversive, area. An aperture of 5 × 5 cm with rounded-down corners led from the light area to the dark box. Each mouse was released in the dark compartment and observed for 5 min. Coat state was scored on the head, neck, back and ventrum with either a zero for a normally groomed coat or a 1 for an unkempt coat at each site. The elevated-plus-maze test was performed with a maze consisting of two side-shielded arms and two open arms (height, 40 cm). Mice were placed into the central area, and behavior was tested for 5 min. In the splash test, 200 µL of a 10% sucrose solution was spotted onto the mouse's snout, and the latency to begin grooming and the grooming frequency over 5 min were measured. Control experiments showed that the different genotypes did not differ in their locomotion.

Egg-laying assay. *asm-1*(kk-1) worms and WT *C. elegans* Bristol strain (N2) worms (from Caenorhabditis Genetics Center, University of Minnesota, Minneapolis, USA) were cultured at 20 °C and fed with *Escherichia coli* OP50 as a food source. Egg laying was counted from young adults that were picked as L4 larvae from OP50 plates and transferred to fresh bacteria plates before the assay. After development for 20 h at 20 °C, worms from these plates were then transferred individually to 96-well microplates containing 50 µL M9 buffer (20 mM KH₂PO₄, 40 mM Na₂HPO₄, 80 mM NaCl, 1 mM MgSO₄) per well with or without 1 mM fluoxetine or 12.5 mM 5-hydroxytryptamine. The number of eggs released was scored after 90 min at room temperature. Each assay contained six to eight worms for each experimental group.

Hippocampal ceramide injection and behavior. Adult male C57BL/6 mice (Charles River, Germany) were deeply anesthetized with 1 g per kg body weight ketamine and 76 mg per kg body weight medetomidine hydrochloride intraperitoneally and 100 mg per kg body weight metamizol subcutaneously. The mouse was placed in a Kopf stereotaxic frame. Two injection cannulas (Microbiotech/se AB, Stockholm, Sweden) were aimed at the dorsal hippocampus (AP -2.0; ML ± 1.5; DV -2.3 mm) using coordinates relative to bregma and fixed in place using two anchor screws (stainless steel, diameter 1.4 mm) and dental cement. Mice were kept warm and allowed to recover from anesthesia. Mice were then returned to their home cage for single housing and monitored daily, allowing at least 4 d for complete recovery. All mice received seven bilateral injections with either 2 µM C16 ceramide (Cayman, Ann Arbor, USA) or ghost micelles. C16 ceramide solution was prepared in 2% octyl β-D-glucopyranoside and sonicated for 10 min before use. The ceramide test dose was determined after a dose-response test (2–200 µM). In that test, 2 µM ceramide had no acute adverse effects on behavior. All injections were spaced 48 h apart. The injection volume was 0.2 µL per side, delivered at a flow rate of 0.1 µL min⁻¹. After injection, cannulas were left in place for 1 min to allow for diffusion. After the seventh injection, coat state was scored and one day later, novelty-suppressed feeding was tested as described above. Then mice received two more ceramide injections spaced 48 h apart before sucrose preference was tested on four consecutive days. Each mouse received two bottles constantly available, one filled with a 2% sucrose solution and one with water. Percentage preference of sucrose versus water was measured every day. After the behavioral tests, mice were killed by cervical dislocation, and brains were removed for verification of probe localization^{37,38}.

Statistical analyses. Data were examined with analysis of variance (ANOVA) and *post hoc* tests. A *P* value of 0.05 or less (two-tailed *t*-test) was considered indicative of statistical significance.

34. Horinouchi, K. *et al.* Acid sphingomyelinase deficient mice: a model of types A and B Niemann-Pick disease. *Nat. Genet.* **10**, 288–293 (1995).
35. Lozano, J. *et al.* Niemann-Pick disease versus acid sphingomyelinase deficiency. *Cell Death Differ.* **8**, 100–103 (2001).
36. Lakso, M. *et al.* Efficient *in vivo* manipulation of mouse genomic sequences at the zygote stage. *Proc. Natl. Acad. Sci. USA* **93**, 5860–5865 (1996).
37. Amato, D., Müller, C.P. & Badiani, A. Increased drinking after intra-striatal injection of the dopamine D2/D3 receptor agonist quinpirole in the rat. *Psychopharmacology (Berl.)* **223**, 457–463 (2012).
38. Franklin, K.B.J. & Paxinos, G. *The Mouse Brain in Stereotaxic Coordinates* 3rd edn., Figure 48 (Academic Press, San Diego, 2007).